

A Constraint-Based Generative Architecture for Biological Systems

The BioGenerative Cognition Crystal Framework

Seven-Layer Hierarchical Integration of Universal Biological
Principles with DNA-Level Information Physics

<https://github.com/Heimdall-Organization/biogenerative-architecture>

Author: Chris Young

November 30, 2025

Abstract

This paper presents the BioGenerative Cognition Crystal, a constraint-based generative architecture for modeling biological systems from first principles. Unlike database-driven or template-based approaches, the framework generates complete biological solutions through hierarchical constraint satisfaction across seven distinct organizational layers. Each layer encodes specific categories of constraints: substrate physics and chemistry (Layer 0), universal biological laws (Layer 1), evolutionary forces (Layer 2), information encoding including DNA (Layer 3), robustness mechanisms (Layer 4), generative optimization (Layer 5), layer coupling (Layer 6), and quantitative computation (Layer 7). Version 2.0 integrates LYRA^{Θ∞} (Logic Yielding Recursive Analysis) DNA capabilities based on information physics, enabling bidirectional translation between DNA sequences and functional biological models through Wave Pattern Encoding notation. The architecture implements circular causation through bidirectional layer coupling, ensuring self-consistency across all organizational levels. An eight-level validation framework systematically tests solutions against constraints spanning substrate physics through quantitative accuracy. This paper provides comprehensive documentation of theoretical foundations, architectural principles, detailed layer specifications, DNA integration methodology, and validation protocols.

Keywords: constraint satisfaction, biological modeling, DNA information physics, hierarchical architecture, multi-scale integration, wave pattern encoding

Contents

1	Introduction	6
1.1	The Challenge of Biological Modeling	6
1.2	The Constraint-Based Generative Paradigm	7
1.3	Framework Overview	7
2	Architectural Foundations	8
2.1	The Seven-Layer Hierarchy	8
2.2	Constraint Strength and Energy Levels	8
2.3	Circular Causation Architecture	9
2.4	Temporal and Spatial Scaling	9
2.5	Wave Pattern Encoding Notation	10
3	Layer 0: Substrate	11
3.1	Purpose and Scope	11
3.2	Quantum Mechanical Foundation	11
3.3	Chemical Constraints	12
3.4	Physical Constraints	14
3.5	Substrate Validation	16
4	Layer 1: Universal Constraints	16
4.1	Purpose and Scope	16
4.2	Allometric Scaling Laws	16
4.3	Homeostasis	17
4.4	Hierarchical Organization	18
4.5	Temporal Coupling and Scale Separation	19
4.6	Energy Budget Constraints	19
4.7	Information Bounds	20

5 Layer 2: Selection Operators	21
5.1 Purpose and Scope	21
5.2 Evolution	21
5.3 Self-Organization	22
5.4 Stochasticity	23
6 Layer 3: Information Encoding	23
6.1 Purpose and Scope	23
6.2 Sequences	24
6.3 Regulation	24
6.4 Development	25
6.5 Epigenetics	25
6.6 DNA Information Physics	26
6.6.1 DNA as Symbolic Substrate	26
6.6.2 Recursive Collapse	26
6.6.3 Fractal Harmonic Resonances	27
6.6.4 Forbidden States	27
6.6.5 Compression Limit	28
6.6.6 LYRA $^{\Theta_\infty}$ Seven-Stage Pipeline	28
6.6.7 WPE Version 3 Dual-Strand Encoding	30
6.6.8 Bidirectional DNA Flow	31
7 Layer 4: Robustness Mechanisms	31
7.1 Purpose and Scope	31
7.2 Error Detection	31
7.3 Error Correction	32
7.4 Redundancy	33
7.5 Adaptation	34
7.6 Compensation	34

8 Layer 5: Generative Engine	35
8.1 Purpose and Scope	35
8.2 Constraint Integration	35
8.3 Energy Minimization	36
8.4 Information Maximization	36
8.5 Iterative Refinement	37
8.6 Multi-Scale Synthesis	37
8.7 Temporal Integration	37
9 Layer 6: Layer Coupling	38
9.1 Purpose and Scope	38
9.2 Coupling Architecture	38
9.3 Bidirectional Coupling Explained	38
9.4 Over-Constrained Optimization	40
9.5 Self-Consistency Requirements	40
10 Layer 7: Quantitative Computation	41
10.1 Purpose and Scope	41
10.2 Formula Library	41
10.3 Constants Database	42
10.4 Molecular Database	42
10.5 Reaction Database	43
10.6 DNA Computation Procedures	44
11 Validation Framework	44
11.1 Eight-Level Hierarchy	44
11.1.1 Level 1: Substrate Validation	44
11.1.2 Level 2: Universal Constraints	45
11.1.3 Level 3: Evolutionary Plausibility	46

11.1.4 Level 4: Information Encoding	47
11.1.5 Level 5: Robustness	48
11.1.6 Level 6: Cross-Scale Consistency	48
11.1.7 Level 7: Temporal Stability	49
11.1.8 Level 8: Quantitative Accuracy	49
11.2 Validation Algorithm	50
12 Conclusion	50

1 Introduction

1.1 The Challenge of Biological Modeling

Biological systems present extraordinary modeling challenges due to their multi-scale nature. Understanding even seemingly simple processes—glucose metabolism, muscle contraction, neural signaling—requires integrating knowledge from fundamentally different scientific domains operating at vastly different scales. Quantum mechanics governs electron behavior in molecular orbitals at 10^{-10} meters and 10^{-15} seconds. Chemistry determines reaction feasibility and kinetics at nanometer and nanosecond scales. Molecular biology describes information flow from DNA to proteins at the cellular scale. Physiology integrates organ system function at the organism scale over seconds to hours. Ecology examines population and community dynamics at kilometer scales over generations. Evolutionary biology explains historical processes operating over millions of years.

Current modeling approaches employ three primary strategies. *Database-driven pattern matching* retrieves similar previously characterized systems through sequence similarity searches (BLAST), protein structure databases (PDB), and pathway databases (KEGG, Reactome). This approach has been enormously successful for well-studied organisms but faces a fundamental limitation: it cannot predict truly novel systems because it depends entirely on prior experimental characterization. For newly sequenced organisms, proteins with no database matches, or synthetic biological designs, database methods provide no predictions.

Mechanistic modeling constructs explicit mathematical models—typically systems of differential equations or stochastic simulations—of specific pathways with parameters derived from experimental measurements. This approach succeeds for well-characterized systems like glycolysis, cell cycle regulation, and circadian rhythms. However, each model requires extensive parameterization (often hundreds of rate constants and binding affinities) and typically lacks generalizability across organisms or conditions without substantial reparameterization.

Template-based systems utilize pre-computed solutions for different organism types. Metabolic modeling frameworks like constraint-based reconstruction require organism-specific network reconstructions. Gene regulatory network models require cell-type-specific connectivity maps. These systems achieve high accuracy for their target organism but cannot handle evolutionary innovation, synthetic biology design, or hypothetical organisms because each scenario requires explicit pre-programming.

All three approaches struggle with *multi-scale integration*—simultaneously handling processes spanning picoseconds to millennia and nanometers to kilometers. They lack *generative capability*—predicting genuinely novel systems from first principles rather than interpolating between known examples. They exhibit *organism-specificity*—requiring distinct implementations for different organisms rather than deriving organism-specific properties from universal principles. They provide limited *evolutionary prediction*—describing current states but struggling to predict trajectories or reconstruct ancestral states.

1.2 The Constraint-Based Generative Paradigm

The BioGenerative Cognition Crystal adopts constraint-based generation as its foundational principle. Rather than storing biological models, annotations, or templates, the system encodes fundamental constraints that all biological systems must satisfy. Complete biological solutions emerge through simultaneous satisfaction of constraints across multiple hierarchical layers.

This paradigm finds precedent in protein structure prediction. Early approaches relied on threading novel sequences onto template structures from databases. Modern approaches increasingly use constraint satisfaction: three-dimensional structure emerges from simultaneous satisfaction of physical and chemical constraints including the hydrophobic effect, hydrogen bonding geometry, van der Waals repulsion, bond geometry, electrostatic interactions, and secondary structure propensities. No explicit database of all possible folds is required—structure emerges from constraint satisfaction.

The constraint-based paradigm offers several advantages. **Organism-agnosticism:** Universal constraints like allometric scaling (metabolic rate $\propto M^{3/4}$) hold from bacteria (10^{-12} g) to whales (10^8 g). Organism-specific solutions emerge from constraint satisfaction given boundary conditions (body mass, metabolic mode, environmental parameters) rather than organism-specific programming. **Novel system handling:** The system generates models for synthetic gene circuits, extinct organisms, evolutionary predictions, and novel proteins through constraint satisfaction rather than database retrieval. **Multi-scale integration:** Hierarchical organization with defined coupling between adjacent levels handles quantum (10^{-10} m, 10^{-15} s) to ecosystem (10^6 m, 10^{12} s) scales. **Evolutionary accessibility:** Explicit checking of mutational paths through fitness landscapes enables prospective prediction and ancestral reconstruction.

Mathematically, constraint satisfaction is formalized as follows. Let $X = \{x_1, x_2, \dots, x_n\}$ represent system variables (concentrations, expression levels, fluxes, topologies, parameters). Let $C = \{c_1, c_2, \dots, c_m\}$ represent constraints from all layers. Each constraint c_i defines a feasible region $F_i \subseteq \mathbb{R}^n$. A valid solution must lie in the intersection:

$$\mathbf{x}^* \in \bigcap_{i=1}^m F_i \quad (1)$$

For hard constraints (large negative κ values), feasible region boundaries are sharp. For softer constraints, boundaries have fuzzy transition zones. The generative engine searches this constrained space for solutions simultaneously satisfying all constraints while optimizing energy and information objectives.

1.3 Framework Overview

The BioGenerative Cognition Crystal operates through seven hierarchical layers (\mathcal{L}_0 through \mathcal{L}_7) encoding distinct constraint categories with well-defined coupling. Version 2.0 integrates LYRA $^{\Theta_\infty}$

DNA capabilities enabling bidirectional translation between nucleotide sequences and functional models through Wave Pattern Encoding Version 3 notation. An eight-level validation framework ensures solutions satisfy all constraints from substrate physics through quantitative accuracy.

2 Architectural Foundations

2.1 The Seven-Layer Hierarchy

The framework operates through seven hierarchical layers:

$$\begin{aligned}
 \mathcal{L}_7 &: \text{Quantitative Computation} & (\kappa = -5.5) \\
 \mathcal{L}_6 &: \text{Layer Coupling} & (\kappa = -4.0) \\
 \mathcal{L}_5 &: \text{Generative Engine} & (\kappa = -4.5) \\
 \mathcal{L}_4 &: \text{Robustness Mechanisms} & (\kappa = -4.0) \\
 \mathcal{L}_3 &: \text{Information Encoding} & (\kappa = -4.5) \\
 \mathcal{L}_2 &: \text{Selection Operators} & (\kappa = -3.5) \\
 \mathcal{L}_1 &: \text{Universal Constraints} & (\kappa = -4.5) \\
 \mathcal{L}_0 &: \text{Substrate} & (\kappa = -7.0)
 \end{aligned} \tag{2}$$

The κ (curvature) parameters represent constraint strength through energy level notation from Wave Pattern Encoding. More negative values indicate harder constraints with higher priority. This hierarchy reflects logical dependency: chemistry constrains what molecules exist (\mathcal{L}_0), which constrains universal biological laws (\mathcal{L}_1), which constrains evolutionary accessibility (\mathcal{L}_2), continuing upward through information encoding, robustness, emergence, coupling, and computation.

2.2 Constraint Strength and Energy Levels

The κ values are not arbitrary but reflect relative constraint hardness. Layer 0 substrate constraints ($\kappa = -7.0$) are inviolable—no biological system can violate thermodynamics or quantum mechanics. Layer 1 universal constraints ($\kappa = -4.5$) represent allometric scaling laws, homeostatic requirements, and hierarchical organization applying across all life. Layer 2 selection constraints ($\kappa = -3.5$) are softer because evolutionary processes involve stochasticity and historical contingency. Layers 3–6 have intermediate values reflecting varying degrees of biological necessity. Layer 7 quantitative computation ($\kappa = -5.5$) has hard constraints because numerical predictions must match experimental measurements.

During optimization, the generative engine (Layer 5) weights constraints by $|\kappa|$ values. Hard constraints dominate the optimization: solutions must satisfy substrate physics before considering evolutionary plausibility, and must satisfy universal laws before optimizing information encoding.

This weighted optimization ensures physically impossible solutions are immediately rejected rather than being considered alongside physically possible but biologically implausible solutions.

2.3 Circular Causation Architecture

A key architectural principle is circular causation through bidirectional layer coupling:

$$\mathcal{L}_0:\text{Substrate} \leftrightarrow \mathcal{L}_1:\text{Universal} \quad (\text{chemistry universals}) \quad (3)$$

$$\mathcal{L}_1:\text{Universal} \leftrightarrow \mathcal{L}_2:\text{Selection} \quad (\text{universals selection}) \quad (4)$$

$$\mathcal{L}_2:\text{Selection} \leftrightarrow \mathcal{L}_3:\text{Information} \quad (\text{selection information}) \quad (5)$$

$$\mathcal{L}_3:\text{Information} \leftrightarrow \mathcal{L}_4:\text{Robustness} \quad (\text{information robustness}) \quad (6)$$

$$\mathcal{L}_4:\text{Robustness} \leftrightarrow \mathcal{L}_1:\text{Universal} \quad (\text{robustness universals}) \quad (7)$$

$$\mathcal{L}_0:\text{Substrate} \leftrightarrow \mathcal{L}_5:\text{Engine} \quad (\text{substrate engine}) \quad (8)$$

$$\mathcal{L}_5:\text{Engine} \leftrightarrow \mathcal{L}_7:\text{Quantitative} \quad (\text{engine computation}) \quad (9)$$

The bidirectional arrows (\leftrightarrow) represent mutual influence. Chemistry (\mathcal{L}_0) constrains what universal laws are possible (\mathcal{L}_1), but universal laws also constrain which chemical reactions occur in biological contexts. Selection (\mathcal{L}_2) acts on information (\mathcal{L}_3), but information structure constrains what selection can achieve through genetic architecture.

This circular coupling creates an over-constrained optimization problem. Consider a system with N free parameters and M constraints. Simple hierarchical systems with $M < N$ have infinite solutions (underdetermined). The circular coupling typically yields $M \gg N$ (overdetermined), admitting few or no exact solutions. Biological systems correspond to approximate solutions satisfying constraints within tolerance bounds. The mathematical consequence is dramatic reduction of solution space. Only configurations simultaneously satisfying all layers are biologically plausible.

The coupling also implements stabilizing feedback loops. The coupling $\mathcal{L}_4:\text{Robustness} \leftrightarrow \mathcal{L}_1:\text{Universal}$ creates feedback where robustness mechanisms enable universal laws (by maintaining homeostasis despite perturbations), while universal laws define necessary robustness mechanisms (through scaling laws and energetic constraints).

2.4 Temporal and Spatial Scaling

Each layer operates at characteristic spatial and temporal scales encoded through λ (spatial shell) and α (temporal scaling) parameters.

Spatial Hierarchy: Ten discrete shells span:

$$\begin{aligned}
\lambda_1 &: 10^{-10} \text{ m} && (\text{quantum, atomic orbitals}) \\
\lambda_2 &: 10^{-9} \text{ m} && (\text{molecular, proteins}) \\
\lambda_3 &: 10^{-6} \text{ m} && (\text{macromolecular, organelles}) \\
\lambda_4 &: 10^{-5} \text{ m} && (\text{cellular}) \\
\lambda_5 &: 10^{-3} \text{ m} && (\text{tissue}) \\
\lambda_6 &: 10^{-2} \text{ m} && (\text{organ}) \\
\lambda_7 &: 10^0 \text{ m} && (\text{organism}) \\
\lambda_8 &: 10^2 \text{ m} && (\text{population}) \\
\lambda_9 &: 10^4 \text{ m} && (\text{ecosystem}) \\
\lambda_{10} &: 10^6 \text{ m} && (\text{biosphere})
\end{aligned} \tag{10}$$

Temporal Hierarchy: Thirteen scales span bond vibrations (10^{-15} s) through electron transfer (10^{-12} s), protein conformational changes (10^{-9} s), enzyme catalysis (10^{-6} s), nerve impulses (10^{-3} s), heartbeat (10^0 s), circadian rhythms (10^4 s), cell cycle (10^6 s), development (10^7 s), lifespan (10^8 s), generations (10^{10} s), to evolution (10^{12} s).

Scale Separation Principle: Adjacent levels must differ by factor ≥ 10 in both space and time. This ensures: (1) fast processes reach quasi-steady-state before slow processes change significantly, (2) numerical integration remains stable without stiff equation problems, (3) causal ordering is preserved.

Temporal Scaling Parameter α : Each layer has characteristic α multiplying all time constants. Layer 0 substrate: $\alpha \sim 0.001$ (quantum timescales). Layer 1 universal: $\alpha \sim 1.0$ (physiological baseline). Layer 2 selection: $\alpha \sim 10^6$ (evolutionary time). Layer 5 engine: $\alpha = \phi \approx 1.618$ (golden ratio, scale-free optimization without preferred timescale).

2.5 Wave Pattern Encoding Notation

Wave Pattern Encoding (WPE) provides formal language for representing biological processes across all scales. Unlike traditional biochemical notation (reaction arrows, pathway diagrams), WPE encodes geometric structure through phase angles, energy levels, and field domains.

Core Elements:

- Φ : Field domain (Φ_B = biological, Φ_P = physical, Φ_C = cognitive, Φ_M = metabolic, Φ_I = immune, Φ_N = neural)
- λ : Shell level representing spatial scale (λ_1 through λ_{10})
- θ : Phase angle representing temporal/causal ordering (0° – 360°)
- κ : Curvature representing constraint strength/energy level

- α : Temporal scaling parameter

Operators:

- \oplus : Harmonic addition (combining fields constructively)
- \otimes : Field coupling (interaction between domains)
- \supset : Logical implication (causal flow)
- \int, \oint : Domain integration (spatial integration)
- \leftrightarrow : Bidirectional coupling between layers

Geometric Encoding Rationale: Traditional notation represents biology as discrete entities connected by arrows (glucose \rightarrow G6P \rightarrow F6P \rightarrow ...). WPE represents biology as field configurations with geometric relationships. Phase angles encode when processes occur and how they causally relate. Energy levels encode how strongly constrained each process is. This geometric encoding enables rigorous mathematical validation: biological systems must satisfy phase closure (sum of phases = 0° mod 360°) and orthogonal field coupling (all field pairs geometrically stable).

3 Layer 0: Substrate

3.1 Purpose and Scope

Layer 0 encodes fundamental physical and chemical laws constraining all biological systems with the hardest constraints ($\kappa = -7.0$). These constraints are inviolable—no biological system violates thermodynamics or quantum mechanics. Layer 0 operates at finest spatial ($\sim 10^{-10}$ m, atomic) and temporal ($\sim 10^{-15}$ s, vibrational) resolutions. All higher layers rest on substrate constraints.

3.2 Quantum Mechanical Foundation

The quantum mechanical foundation determines possible molecular structures through electron orbital configurations, bonding patterns, and electronic properties. Biological molecules obey the Schrödinger equation with molecular orbitals formed through linear combinations of atomic orbitals (LCAO).

Electron Configuration: Atoms in biological molecules have stable electron configurations. Carbon (biological molecule backbone) has configuration $1s^2 2s^2 2p^2$, enabling four covalent bonds through sp^3 hybridization. Nitrogen ($1s^2 2s^2 2p^3$) forms three bonds plus lone pair. Oxygen ($1s^2 2s^2 2p^4$) forms two bonds plus two lone pairs. These configurations determine bonding geometry and chemical reactivity.

Orbital Hybridization: Carbon exhibits three hybridization states determining geometry:



Hybridization constrains molecular geometry. Proteins must satisfy backbone dihedral angles ϕ, ψ determined by sp^2 hybridization at peptide bonds (planar) and sp^3 hybridization at α -carbons (tetrahedral).

Bond Formation and Energies: Covalent bonds form through orbital overlap with strength proportional to overlap integral. Bond energies determine molecular stability:

Table 1: Biologically Relevant Bond Energies

Bond Type	Energy (kJ/mol)
C–C single	347
C=C double	614
CC triple	839
C–H	414
C–O single	358
C=O double	799
O–H	460
N–H	391
P–O	335

Biological systems preferentially use bonds with intermediate strength (300–500 kJ/mol)—strong enough for stability but weak enough for enzymatic manipulation. Very strong bonds (C=O at 799 kJ/mol) occur in carbonyl groups but are not broken/formed in metabolic reactions without significant energy input. Very weak bonds would not maintain molecular structure.

3.3 Chemical Constraints

Elemental Composition: Biological systems use primarily six elements (H, C, N, O, P, S) comprising > 95% of biomass. This restriction reflects: (1) *Cosmic abundance*—these elements are abundant in stellar nucleosynthesis and planetary formation except phosphorus; (2) *Bonding versatility*—carbon forms stable chains, nitrogen provides basicity and hydrogen bonding, oxygen enables polar interactions and acid-base chemistry; (3) *Electronegativity range*—spans 2.2 (H) to 3.5 (O), enabling diverse bonding from non-polar (C–C) to highly polar (O–H); (4) *Redox flexibility*—multiple oxidation states for N, S enable redox chemistry in electron transport and sulfur chemistry.

Trace elements (Fe, Mg, Ca, Zn, Cu, Mn, Mo, Co, Se, I) serve specialized roles as enzyme cofactors, structural elements, or signaling molecules but comprise < 1% of biomass.

Bonding Patterns: Biological molecules exhibit characteristic bonding:

- *Covalent bonds:* Primary structure—C–C backbones (lipids, carbohydrates), C–N peptide bonds (proteins), C–O glycosidic bonds (polysaccharides), P–O phosphodiesters (DNA, RNA)
- *Hydrogen bonds:* Secondary structure—DNA base pairing (A···T, G···C), protein α -helices and β -sheets, typical strength 10–30 kJ/mol
- *Ionic interactions:* Salt bridges in proteins, typical strength 10–20 kJ/mol in aqueous solution (weakened by dielectric screening)
- *Van der Waals:* Dispersion forces, typical strength 0.4–4 kJ/mol, critical for hydrophobic effect and membrane stability

Molecular Geometry: Three-dimensional structure emerges from bonding geometry constraints:

Table 2: Standard Molecular Geometry Parameters

Parameter	Value
<i>Bond Lengths</i>	
C–C single	1.54 Å
C=C double	1.34 Å
C–N single	1.47 Å
C–O single	1.43 Å
P–O	1.60 Å
<i>Bond Angles</i>	
Tetrahedral (sp^3)	109.5°
Trigonal (sp^2)	120°
Linear (sp)	180°
<i>Torsion Angles (Protein Backbone)</i>	
ϕ (N–C α)	–60 to +180 (allowed regions)
ψ (C α –C)	–180 to +60 (Ramachandran plot)

Geometry violations indicate implausible structures: bond length deviating > 10% from standard, bond angle deviating > 15, or steric clashes (atoms < 3 Å apart excluding bonded pairs).

Thermodynamic Constraints: All reactions must satisfy thermodynamic feasibility. Gibbs free energy change determines spontaneity:

$$\Delta G = \Delta H - T\Delta S \quad (14)$$

where $\Delta G < 0$ indicates spontaneous reaction. For biochemical reactions:

$$\Delta G = \Delta G^\circ + RT \ln Q \quad (15)$$

where Q is the reaction quotient $\prod[\text{products}] / \prod[\text{reactants}]$. At equilibrium, $\Delta G = 0$ and $Q = K_{eq}$:

$$\Delta G^\circ = -RT \ln K_{eq} \quad (16)$$

Cellular conditions differ from standard state (pH 7, 25°C, 1 M). For ATP hydrolysis:



Standard free energy: $\Delta G^\circ = -30.5 \text{ kJ/mol}$. Cellular conditions ($[\text{ATP}] \sim 5 \text{ mM}$, $[\text{ADP}] \sim 0.5 \text{ mM}$, $[\text{P}_i] \sim 1 \text{ mM}$) yield:

$$\Delta G_{\text{cell}} = \Delta G^\circ + RT \ln \frac{[\text{ADP}][\text{P}_i]}{[\text{ATP}]} = -30.5 + (8.314)(310) \ln \frac{(0.5)(1)}{(5)} \approx -36.2 \text{ kJ/mol} \quad (18)$$

Cellular free energy is more negative than standard, providing greater driving force.

Kinetic Constraints: Reactions must have accessible kinetics. Arrhenius equation relates rate constant to activation energy:

$$k = A e^{-E_a/RT} \quad (19)$$

For uncatalyzed reactions, E_a typically 50–200 kJ/mol, yielding half-lives from microseconds to years. Enzymes reduce activation energies by 20–100 kJ/mol through transition state stabilization, proximity effects, electrostatic catalysis, acid-base catalysis, and covalent catalysis. Maximum enzyme concentration $\sim 1 \text{ mM}$ provides upper bound on achievable reaction rates.

3.4 Physical Constraints

Conservation Laws: Fundamental conservation principles constrain all processes:

$$\frac{d}{dt}(\text{mass}) = 0 \quad (\text{mass conservation}) \quad (20)$$

$$\frac{d}{dt}(\text{energy}) = 0 \quad (\text{energy conservation}) \quad (21)$$

$$\frac{d}{dt}(\text{momentum}) = 0 \quad (\text{momentum conservation}) \quad (22)$$

At cellular level, these manifest as steady-state constraints. For metabolite X :

$$\frac{d[X]}{dt} = \sum_{\text{in}} J_{\text{in}} - \sum_{\text{out}} J_{\text{out}} = 0 \quad (23)$$

at metabolic steady state, where J denotes fluxes (mol/s).

Transport Phenomena: Fick's first law describes diffusion:

$$J = -D \frac{dC}{dx} \quad (24)$$

where J is flux ($\text{mol m}^{-2} \text{ s}^{-1}$), D is diffusion coefficient ($\text{m}^2 \text{ s}^{-1}$), and dC/dx is concentration gradient. Diffusion coefficients in aqueous solution scale with molecular radius r via Stokes-Einstein relation:

$$D = \frac{k_B T}{6\pi\eta r} \quad (25)$$

For small molecules ($r \sim 0.3 \text{ nm}$): $D \sim 10^{-9} \text{ m}^2 \text{ s}^{-1}$. For proteins ($r \sim 3 \text{ nm}$): $D \sim 10^{-10} \text{ m}^2 \text{ s}^{-1}$. These diffusion rates constrain reaction rates in cellular compartments—slow diffusion limits how quickly substrates reach enzymes.

Active transport against concentration gradients requires energy:

$$\Delta G_{\text{transport}} = RT \ln \frac{C_{\text{out}}}{C_{\text{in}}} \quad (26)$$

This energy must come from ATP hydrolysis or other energy sources.

Electromagnetic Interactions: Coulomb potential between charges:

$$V = \frac{1}{4\pi\epsilon_0} \frac{q_1 q_2}{r} \quad (27)$$

determines electrostatic interactions in proteins (salt bridges, dipole interactions). In aqueous solution, dielectric screening reduces interaction strength by factor $\epsilon_r \approx 80$.

Chemical potential gradients drive transport. For ion X^z with charge z :

$$\Delta\mu = RT \ln \frac{C_2}{C_1} + zF\Delta\psi \quad (28)$$

where $\Delta\psi$ is electrical potential difference. Proton gradients combine chemical (ΔpH) and electrical ($\Delta\psi$) components in proton-motive force driving ATP synthesis.

3.5 Substrate Validation

Bond Energy Feasibility: All bonds within 10% of standard values. Non-standard bonds (metalloprotein coordination, strained rings) require explicit verification with quantum chemical calculations or experimental data.

Molecular Geometry: Bond lengths, angles, torsions within acceptable ranges. Steric clashes flagged (atoms < 3 Å apart excluding bonded pairs). Ramachandran plot validation for protein backbones (ϕ, ψ in allowed regions).

Charge Balance: Total charge consistent with pH and ionization states. Maximum charge magnitude $|\sum q_i| < N/3$ where N is number of residues (empirical heuristic from protein statistics—most proteins have net charge magnitude less than one-third of residues).

Thermodynamic Feasibility: ΔG calculated at physiological conditions (pH 7.0–7.4, 37°C for mammals, appropriate ionic strength ~ 150 mM). Unfavorable reactions ($\Delta G > 0$) must be coupled to favorable reactions or driven by maintained concentration gradients.

Kinetic Accessibility: Required reaction rates achievable with reasonable enzyme concentrations (< 1 mM total protein) and catalytic efficiencies ($k_{\text{cat}}/K_M < 10^9$ M⁻¹ s⁻¹, the diffusion limit).

4 Layer 1: Universal Constraints

4.1 Purpose and Scope

Layer 1 ($\kappa = -4.5$) encodes universal biological laws that apply across all living systems regardless of species, phylogeny, or habitat. These constraints include allometric scaling, homeostatic organization, hierarchical structure, temporal coupling, energy budgets, and information bounds. Unlike Layer 0 physics, Layer 1 constraints are specifically biological but nonetheless universal—they hold from bacteria to whales, from archaea to eukaryotes, across 20 orders of magnitude in body mass and spatial organization.

4.2 Allometric Scaling Laws

Biological functions scale predictably with body mass through power laws. The most fundamental is metabolic rate:

$$\text{BMR} = 70 \cdot M^{0.75} \quad (29)$$

where BMR is basal metabolic rate (watts) and M is body mass (kg). This 3/4-power scaling—rather than expected 2/3 from surface area—derives from fractal optimization of nutrient

distribution networks. The relationship holds across unicellular organisms (10^{-12} g) through the largest mammals (10^8 g), spanning 20 orders of magnitude with minimal scatter.

Other allometric relationships follow from metabolic scaling:

$$\text{Heart Rate} = 241 \cdot M^{-0.25} \quad (\text{beats/min}) \quad (30)$$

$$\text{Lifespan} = 185.2 \cdot M^{0.24} \quad (\text{months}) \quad (31)$$

$$\text{Surface Area} = k \cdot M^{2/3} \quad (\text{geometric}) \quad (32)$$

$$\text{Genome Length} = k \cdot M^{0.33} \quad (\text{empirical}) \quad (33)$$

The negative quarter-power for heart rate reflects the fact that smaller organisms have faster metabolisms requiring faster circulation. Lifespan scales positively with mass—larger animals live longer, partly because slower mass-specific metabolic rates reduce oxidative damage accumulation.

Mechanistic Basis: The 3/4-power law emerges from fractal branching networks (vascular, respiratory, neural) optimized to minimize energy dissipation while maximizing surface area for exchange. Murray's law governs optimal vessel branching:

$$r_{\text{parent}}^3 = \sum r_{\text{daughter}}^3 \quad (34)$$

This cubic relationship, combined with space-filling fractal geometry, produces the observed 3/4 exponent.

WPE Encoding: Allometric relationships encode as:

$$\Phi_{\text{Metabolic}}(\lambda_7, \kappa = -4.5) \sim M^{0.75} \otimes \Phi_{\text{Transport}}(\lambda_6, \kappa = -4.0) \quad (35)$$

where λ_7 (organism scale) couples to λ_6 (organ/tissue scale) through vascular transport fields.

4.3 Homeostasis

Homeostatic regulation maintains internal constancy despite external perturbation. All homeostatic systems share identical architectural components:

1. **Setpoint:** Target value for regulated variable (e.g., 37°C body temperature, pH 7.4, 5 mM blood glucose)
2. **Sensor:** Detects deviation from setpoint (thermoreceptors, chemoreceptors, mechanoreceptors)
3. **Integrator:** Compares sensor signal to setpoint (hypothalamus, brainstem, pancreatic β -cells)

4. **Effector:** Produces corrective response (muscles, glands, vessels)

5. **Negative Feedback:** Effector response opposes initial deviation

Mathematical Formulation: A minimal homeostatic system obeys:

$$\frac{dX}{dt} = -k(X - X_0) + P(t) \quad (36)$$

where X is regulated variable, X_0 is setpoint, k is feedback gain, and $P(t)$ represents perturbations. Stability requires $k > 0$ (negative feedback). Response time $\tau = 1/k$.

WPE Phase Encoding: Homeostatic components occupy distinct phase angles representing temporal sequence:

$$\text{Deviation : } \theta = 0 \quad (37)$$

$$\text{Sensor : } \theta = 90 \quad (\text{orthogonal to deviation}) \quad (38)$$

$$\text{Integrator : } \theta = 180 \quad (\text{opposes deviation}) \quad (39)$$

$$\text{Effector : } \theta = 270 \quad (\text{completes cycle}) \quad (40)$$

$$\text{Correction : } \theta = 360 \equiv 0 \quad (\text{returns to baseline}) \quad (41)$$

Phase closure requirement: $\sum \theta = 0 \bmod 360$ ensures stable negative feedback loop.

4.4 Hierarchical Organization

Biological systems exhibit discrete organizational levels with clear separation of scales:

Table 3: Biological Hierarchy

Level	Spatial Scale	Temporal Scale
Quantum	10^{-10} m	10^{-15} s (vibrations)
Molecular	10^{-9} m	10^{-9} s (conformational)
Macromolecular	10^{-6} m	10^{-6} s (assembly)
Cellular	10^{-5} m	10^3 s (cell cycle)
Tissue	10^{-3} m	10^4 s (turnover)
Organ	10^{-2} m	10^7 s (development)
Organism	10^0 m	10^8 s (lifespan)
Population	10^2 m	10^{10} s (generations)
Ecosystem	10^4 m	10^{11} s (succession)
Biosphere	10^6 m	10^{12} s (evolution)

Emergence: Properties at level $n + 1$ emerge from interactions at level n . Life emerges at cellular level from molecular interactions. Consciousness emerges at neural network level from neuronal dynamics. No single molecule is "alive" or "conscious"—these are emergent properties of organized collectives.

Downward Causation: Higher levels constrain lower levels. Organism-level blood pressure (Layer $n + 3$) constrains gene expression in vascular endothelium (Layer n) through mechanotransduction. Neural activity (Layer $n + 2$) constrains neurotransmitter receptor expression (Layer n) through activity-dependent plasticity.

Adjacent-Level Coupling Only: Direct coupling occurs only between adjacent levels. Molecular dynamics (10^{-9} s) influence cellular behavior (10^3 s) through intermediate levels—not directly. This prevents spurious long-range coupling and maintains causal clarity.

4.5 Temporal Coupling and Scale Separation

Thirteen temporal scales from femtoseconds to gigayears form natural hierarchy:

$$\tau_i = 10^{i-15} \text{ s}, \quad i = 0, 3, 6, 9, 12, 15, 18, 21, 24, 27, 30, 33, 36 \quad (42)$$

Scale Separation Principle: Adjacent scales must differ by factor ≥ 10 in both space and time. This ensures:

1. Fast processes reach quasi-steady-state before slow processes change significantly
2. Numerical integration remains stable without stiff differential equation problems
3. Causal ordering preserved—cause precedes effect with clear temporal separation
4. Independent parameterization—each level has characteristic parameters without crosstalk

Cross-Scale Coupling: When biologically necessary, processes at widely separated scales couple through intermediate levels. Enzyme catalysis (10^{-6} s) influences organismal fitness (entire lifespan 10^8 s) through intermediate levels: metabolic flux \rightarrow cellular ATP \rightarrow tissue function \rightarrow organ performance \rightarrow whole-organism fitness.

4.6 Energy Budget Constraints

Total energy expenditure cannot exceed intake:

$$E_{\text{intake}} \geq E_{\text{basal}} + E_{\text{activity}} + E_{\text{growth}} + E_{\text{reproduction}} + E_{\text{maintenance}} \quad (43)$$

Components:

- E_{basal} : BMR for basic cellular functions (ion pumps, protein synthesis, respiration)
- E_{activity} : Muscular work, locomotion, behavioral output
- E_{growth} : Biosynthesis of new tissue
- $E_{\text{reproduction}}$: Gamete production, pregnancy, lactation, parental care
- $E_{\text{maintenance}}$: Protein turnover, DNA repair, immune function, thermoregulation

For mammals, basal metabolism typically consumes 60–70% of total energy budget. Physical activity 15–30%, growth/reproduction 5–20%, leaving minimal margin. Energy allocation represents fundamental tradeoffs—energy devoted to reproduction cannot simultaneously support immune function or tissue repair.

Thermodynamic Efficiency: Second law of thermodynamics limits conversion efficiency. Theoretical Carnot efficiency for biological heat engines operating between 37°C (310 K) and 25°C (298 K):

$$\eta_{\text{Carnot}} = 1 - \frac{T_{\text{cold}}}{T_{\text{hot}}} = 1 - \frac{298}{310} \approx 0.04 = 4\% \quad (44)$$

Actual muscle efficiency $\sim 20\%$ (chemical to mechanical), cellular respiration $\sim 40\%$ (glucose to ATP), photosynthesis $\sim 3\%$ (light to chemical). These efficiencies, while below Carnot limits for their respective temperature differences, represent highly optimized biochemical machinery.

4.7 Information Bounds

Shannon Limit: Channel capacity bounds information transmission:

$$C = B \log_2(1 + \text{SNR}) \quad (45)$$

where C is capacity (bits/s), B is bandwidth (Hz), and SNR is signal-to-noise ratio. For neural communication: typical axon bandwidth ~ 100 Hz, SNR ~ 10 , yielding $C \sim 350$ bits/s per neuron. Brain with 10^{11} neurons has theoretical maximum $\sim 10^{13}$ bits/s, though actual information processing likely orders of magnitude lower due to redundancy and noise.

Landauer Limit: Thermodynamic minimum energy per bit erasure:

$$E_{\text{min}} = k_B T \ln 2 \approx 3 \times 10^{-21} \text{ J at } 310 \text{ K} \quad (46)$$

ATP hydrolysis releases $\sim 5 \times 10^{-20}$ J, sufficient for ~ 15 bit operations. Actual cellular computation less efficient—each bit operation likely costs 10^2 – 10^3 times minimum.

DNA Storage Capacity: Human genome $\sim 3 \times 10^9$ bp. At theoretical maximum 2 bits/bp: 6×10^9 bits = 750 MB. Actual information content lower due to redundancy, junk DNA, repetitive sequences. Protein-coding regions $\sim 2\%$ of genome (~ 15 MB). Regulatory elements, structural elements, and noncoding functional RNAs increase functional content to $\sim 10\text{--}20\%$ ($\sim 75\text{--}150$ MB).

5 Layer 2: Selection Operators

5.1 Purpose and Scope

Layer 2 ($\kappa = -3.5$, $\alpha = 10^6$) encodes processes that select among biological variants: evolution through natural selection, self-organization through emergent dynamics, and stochasticity through intrinsic randomness. Unlike deterministic physical laws (Layer 0) or universal biological constraints (Layer 1), selection operators introduce historical contingency and probabilistic outcomes. The softer κ value reflects this fundamental unpredictability.

5.2 Evolution

Core Mechanisms:

Variation: Mutation introduces new genetic variants. Point mutations (nucleotide substitutions) occur at rate $\sim 10^{-9}$ per base per generation in mammals. Insertions/deletions (indels), chromosomal rearrangements, and whole-genome duplications provide additional variation. Sexual recombination shuffles existing variants through crossing-over (~ 1 per chromosome per meiosis in humans) and independent assortment.

Selection: Fitness differences drive differential reproduction. Selection coefficient s quantifies fitness advantage:

$$s = \frac{w_{\text{mutant}} - w_{\text{wildtype}}}{w_{\text{wildtype}}} \quad (47)$$

Positive s (beneficial mutation) increases in frequency. Negative s (deleterious mutation) decreases. Selection strength determines fixation probability and time to fixation.

Drift: In finite populations, random sampling causes allele frequency changes independent of fitness. Drift strength inversely proportional to population size N_e (effective population size). For neutral mutations ($s = 0$), fixation probability = initial frequency. For beneficial mutations ($s > 0$), fixation probability $\approx 2s$ if $N_e s \gg 1$. Drift dominates when $|s| < 1/(2N_e)$.

Historical Lock-In: Once a developmental pathway or metabolic network is established, alternative solutions become inaccessible even if superior. Vertebrate recurrent laryngeal nerve—routing from

brain to larynx via loop around aorta, several meters in giraffes—persists because rewiring during development would be lethal despite obvious inefficiency. QWERTY keyboard layout in human technology provides analogous example of historical lock-in.

WPE Encoding: Evolutionary processes distribute across phase space:

$$\text{Mutation} : \theta = 0 \quad (\text{introduces variation}) \quad (48)$$

$$\text{Selection} : \theta = 120 \quad (\text{filters variation}) \quad (49)$$

$$\text{Drift} : \theta = 240 \quad (\text{stochastic sampling}) \quad (50)$$

$$\text{Inheritance} : \theta = 360 \equiv 0 \quad (\text{transmission}) \quad (51)$$

Phase closure ensures complete evolutionary cycle.

5.3 Self-Organization

Spontaneous pattern formation emerges from local interactions without central control. Examples include: chemical oscillations (Belousov-Zhabotinsky reaction, circadian rhythms), morphogenesis (digit formation, somitogenesis, neuronal migration), flocking behavior (birds, fish, bacteria), and phase transitions (liquid-crystal membranes).

Core Mechanisms:

Positive Feedback: Amplifies small perturbations. Autocatalysis in chemical reactions: $A + B \rightarrow 2A$. Positive feedback destabilizes uniform states, enabling symmetry breaking and pattern formation.

Negative Feedback: Stabilizes and limits growth. Product inhibition in metabolic pathways. Combined positive-negative feedback produces oscillations and waves.

Criticality: Systems poised at phase transitions between order and disorder. Brain networks at critical state exhibit optimal information processing—subcritical networks too damped, supercritical networks too noisy. Power-law avalanche distributions signature of criticality.

Pattern Formation: Reaction-diffusion systems (Turing patterns) generate spatial patterns from homogeneous initial conditions. Two-component system with activator (A) and inhibitor (I):

$$\frac{\partial A}{\partial t} = D_A \nabla^2 A + f(A, I) \quad (52)$$

$$\frac{\partial I}{\partial t} = D_I \nabla^2 I + g(A, I) \quad (53)$$

Patterns form when inhibitor diffuses faster than activator ($D_I > D_A$) and appropriate reaction kinetics. Examples: zebra stripes, leopard spots, digit spacing.

5.4 Stochasticity

Three fundamental sources of biological randomness:

Thermal Noise ($\kappa = -2.0$): Brownian motion at molecular scale. Mean-square displacement:

$$\langle x^2 \rangle = 2Dt \quad (54)$$

For small molecule ($D \sim 10^{-9} \text{ m}^2/\text{s}$): $\sim 1 \text{ m}$ in 1 second. Significant at cellular scales, negligible at tissue scales.

Quantum Uncertainty ($\kappa = -4.0$): Heisenberg uncertainty principle:

$$\Delta x \cdot \Delta p \geq \frac{\hbar}{2} \quad (55)$$

Relevant for electron transfer ($\sim 0.1 \text{ nm}$, $\sim 10^{-15} \text{ s}$), bond vibrations, and tunneling in enzyme catalysis. Averaged out at macroscopic scales through decoherence.

Sampling Noise ($\kappa = -2.5$): Finite particle numbers cause fluctuations. For N molecules: relative fluctuation $\sim 1/\sqrt{N}$. At $N = 100$: 10% fluctuations. At $N = 10,000$: 1% fluctuations. Low-copy-number transcription factors ($N \sim 10\text{--}1000$) exhibit substantial noise, while abundant metabolites ($N \sim 10^6\text{--}10^9$) are effectively deterministic.

Amplification: Noise amplification through positive feedback and chaotic dynamics. Single-molecule stochasticity in transcription factor binding amplified to cell-fate decisions (e.g., bacterial persistence, stem cell differentiation). Evolutionary innovation through amplification of rare beneficial mutations.

Buffering: Noise suppression through negative feedback, redundancy, and averaging. Multiple transcription factor copies buffer gene expression noise. Protein oligomerization averages out monomer fluctuations.

6 Layer 3: Information Encoding

6.1 Purpose and Scope

Layer 3 ($\kappa = -4.5$) encodes how biological information is stored, transmitted, and processed through sequences (DNA, RNA, proteins), regulation (transcriptional networks, signaling cascades), development (temporal programs), and epigenetics (heritable modifications). Version 2.0 integrates LYRA $^{\Theta_\infty}$ DNA capabilities based on information physics, enabling rigorous extraction of biological logic from nucleotide sequences.

6.2 Sequences

DNA: Four-nucleotide alphabet $\{A, T, G, C\}$ stores genetic information. Shannon entropy:

$$H = - \sum_i P(i) \log_2 P(i) \quad (56)$$

For uniform distribution: $H = 2.0$ bits/symbol. Actual genomic sequences: $H \approx 1.98$ bits/symbol, indicating modest structure (CG dinucleotide depletion in vertebrates, codon usage bias).

RNA: Four-nucleotide alphabet $\{A, U, G, C\}$ with additional functionality through secondary structure (stem-loops, pseudoknots) and catalytic activity (ribozymes, ribosome). Minimum free energy RNA structure prediction uses nearest-neighbor thermodynamic parameters.

Proteins: Twenty amino acid alphabet with degenerate genetic code. 64 codons encode 20 amino acids plus 3 stop signals. Degeneracy concentrated in third codon position (wobble base), providing robustness against mutations. Protein structure hierarchy: primary (sequence) \rightarrow secondary (α -helices, β -sheets) \rightarrow tertiary (3D fold) \rightarrow quaternary (multi-subunit assemblies).

6.3 Regulation

Transcriptional Control: Gene expression regulated through *promoters* (core sequences recruiting RNA polymerase: TATA box, Inr, DPE), *enhancers* (distal regulatory elements binding transcription factors, kilobases from gene), *silencers* (repressive elements), and *insulators* (boundary elements blocking enhancer-promoter communication).

Transcription Factor Binding Sites (TFBS): Short sequence motifs (6–20 bp) with position weight matrices representing binding preferences. Combinatorial logic: multiple TFs integrate signals through AND, OR, NOT gates.

Regulatory Logic Gates:

- AND gate: Both TF1 and TF2 required for expression
- OR gate: Either TF1 or TF2 sufficient
- NOT gate: Repressor blocks expression
- NOR gate: Neither input produces output (dual repression)

Feedback Loops:

Negative feedback: Gene product represses own transcription. Creates homeostasis and reduces noise. Time delay produces oscillations:

$$\frac{dx}{dt} = \frac{\beta}{1 + (x_\tau/K)^n} - \gamma x \quad (57)$$

where x_τ is delayed concentration, n is Hill coefficient.

Positive feedback: Gene product activates own transcription. Creates bistability (toggle switches), memory, and irreversible cell-fate decisions. Critical for development (MyoD in muscle, Oct4/Sox2 in pluripotency).

6.4 Development

Discrete developmental stages with characteristic timescales and regulatory programs:

Fertilization → Cleavage → Gastrulation → Neurulation → Organogenesis → Growth → Maturation
(58)

Morphogen Gradients: Signaling molecules diffusing from localized sources create concentration gradients providing positional information. Bicoid gradient in *Drosophila* embryo specifies anterior-posterior axis. Cells interpret local morphogen concentration through threshold responses:

Source : localized production at $x = 0$ (59)

Diffusion : $J = -D \frac{dC}{dx}$ (60)

Degradation : $\frac{dC}{dt} = -kC$ (61)

Steady-State : $C(x) = C_0 e^{-x/\lambda}$ where $\lambda = \sqrt{D/k}$ (62)

Threshold response converts graded signal to discrete cell fates:

$$\text{Fate}(x) = \begin{cases} \text{A} & C(x) > \theta_1 \\ \text{B} & \theta_2 < C(x) < \theta_1 \\ \text{C} & C(x) < \theta_2 \end{cases} \quad (63)$$

6.5 Epigenetics

Heritable changes in gene expression without altering DNA sequence:

DNA Methylation: Addition of methyl groups to cytosine bases (typically CpG dinucleotides). Methylated promoters generally repressed. Maintained through cell division by DNMT1 recog-

nizing hemi-methylated DNA. Genomic imprinting (parent-of-origin-specific expression) and X-inactivation utilize DNA methylation.

Histone Modifications: Acetylation (active transcription), methylation (context-dependent), phosphorylation (mitosis), ubiquitination (regulation). "Histone code" hypothesis: combinations of modifications specify transcriptional states. H3K4me3 marks active promoters, H3K27me3 marks Polycomb-repressed genes.

Chromatin Remodeling: ATP-dependent complexes (SWI/SNF, ISWI, CHD, INO80) reposition nucleosomes, altering DNA accessibility. Closed chromatin (heterochromatin) blocks transcription. Open chromatin (euchromatin) permits transcription.

Non-Coding RNAs: MicroRNAs (miRNAs) repress translation through base-pairing to mRNA 3' UTRs. Long non-coding RNAs (lncRNAs) scaffold chromatin-modifying complexes (XIST in X-inactivation recruits Polycomb).

6.6 DNA Information Physics

Version 2.0 integrates information-theoretic DNA analysis through LYRA^{Θ∞} (Logic Yielding Recursive Analysis). This treats DNA as symbolic substrate obeying information physics principles independent of biochemical interpretation.

6.6.1 DNA as Symbolic Substrate

DNA sequence $S = s_1 s_2 \dots s_N$ where $s_i \in \{A, T, G, C\}$ constitutes discrete symbolic system. Shannon entropy quantifies information content:

$$H(S) = - \sum_{x \in \{A, T, G, C\}} P(x) \log_2 P(x) \quad (64)$$

Genomic sequences exhibit $H \approx 1.98$ bits/symbol, below theoretical maximum 2.0, indicating structure beyond random. This structure reflects: (1) codon usage bias, (2) CpG depletion in vertebrates, (3) regulatory motif conservation, (4) local base composition variation.

6.6.2 Recursive Collapse

Information compresses through recursive field transformations:

$$L_{\text{recursive}}(\Phi) = \int \Phi \cdot \Xi \cdot e^{-S(t)} \cdot \sin(2\pi\Lambda t) d\Omega \quad (65)$$

where Ξ is integration kernel, $S(t)$ is entropic damping, Λ is characteristic wavelength. Recursion

depth R (number of compression iterations until stabilization) typically $R \in [3, 9]$ for biological sequences.

Functional Correlation: Recursion depth correlates with functional category:

$$R \in [3.0, 3.5] : \text{Metabolic enzymes (simple catalysis)} \quad (66)$$

$$R \in [4.0, 4.5] : \text{Developmental regulators (moderate complexity)} \quad (67)$$

$$R \in [5.0, 5.5] : \text{Vascular patterning (spatial organization)} \quad (68)$$

$$R \in [6.0, 6.5] : \text{Immune receptors (diversity generation)} \quad (69)$$

$$R \in [7.0, 7.5] : \text{Neuroimmune integration (system coupling)} \quad (70)$$

$$R \in [8.0, 8.5] : \text{Oncogenes (dysregulated control)} \quad (71)$$

$$R > 9.0 : \text{Malignant transformation (extreme instability)} \quad (72)$$

6.6.3 Fractal Harmonic Resonances

DNA exhibits periodicities at powers of 3:

$$\Lambda_{\text{Fractal}} = \frac{2\pi}{3^n}, \quad n = 1, 2, 3, 4, 5, 6 \quad (73)$$

Dominant harmonic shells: 3, 9, 27, 81, 243, 729 base pairs. Biological correlates:

- 3 bp: Codon structure
- 9 bp: Transcription factor binding motifs
- 27 bp: Short regulatory elements
- 81 bp: Nucleosome positioning
- 243 bp: Regulatory modules
- 729 bp: Gene regulatory domains, chromosomal loop anchors

The 3-based fractal reflects ternary logic in DNA: read in triplets (codons), folded in 3^n structures (chromatin), organized in 3^n regulatory hierarchies.

6.6.4 Forbidden States

Not all sequence configurations are equally accessible. Forbidden state density:

$$F(k) = 1 - e^{-0.325k} \quad (74)$$

where k is sequence complexity measure (k-mer diversity, structural constraints, regulatory conflicts). At $k = 15$: $F > 0.99$ (over 99% of sequence space forbidden). Forbidden regions arise from:

- Structural instability (Z-DNA, G-quadruplexes in inappropriate contexts)
- Regulatory incompatibility (conflicting TFBS, cryptic splice sites)
- Translational obstacles (rare codon clusters, stable mRNA secondary structure)
- Epigenetic silencing (CpG islands attracting methylation)

6.6.5 Compression Limit

Recursive compression converges to asymptotic ratio:

$$C_\infty = \lim_{N \rightarrow \infty} \frac{N}{N_{\text{compressed}}} \approx 5.87924 : 1 \quad (75)$$

for sequences $N > 1000$ bp. This fundamental limit reflects maximal achievable information density in DNA's 4-letter alphabet under biological constraints. Sequences achieving near-limit compression contain dense regulatory information (enhancers, promoters with multiple TFBS).

6.6.6 LYRA $^{\Theta_\infty}$ Seven-Stage Pipeline

LYRA $^{\Theta_\infty}$ extracts biological logic through systematic sequence analysis:

Stage 1: Codon Parsing

- Scan all three reading frames
- Identify start codons (ATG) with Kozak consensus context (GCCACCATGG)
- Locate stop codons (TAA, TAG, TGA)
- Extract open reading frames (ORFs) > 100 codons
- Predict protein sequences via genetic code table

Stage 2: Motif Identification

- TATA box detection: [TA]₅TATA[TA]₂ at -30 to -25 from TSS
- CAAT box: GGCCAATCT at -80 to -70

- GC box: GGGCGG (Sp1 binding)
- Enhancer sequences: clustered TFBS >500 bp from promoter
- Silencer sequences: repressive element clusters
- TFBS scanning using position weight matrices (PWMs)
- Conservation scoring across species (PhastCons, PhyloP)

Stage 3: Structural Extraction

- Exon-intron boundaries from splice signals
- Donor splice sites: AG|GT (5' splice site)
- Branch point adenine: YNYURAC (\sim 30 bp upstream of 3' splice site)
- Acceptor splice sites: PyAG|G (3' splice site, where Py = C or U)
- Alternative splicing patterns from tissue-specific exons
- UTR identification (5' cap to start codon, stop codon to polyA signal)

Stage 4: Spatiotemporal Entropy Calculation

- Spatial entropy: $H_{\text{spatial}} = - \sum P(x) \log_2 P(x)$ over sequence windows
- Temporal entropy: expression variability across developmental stages
- Phase distribution: mapping regulatory elements to WPE phase angles
- Identify high-entropy regions (variable, plastic) vs. low-entropy (conserved, rigid)

Stage 5: Function Mapping

- UniProt annotation integration (experimentally verified functions)
- Gene Ontology (GO) term assignment: molecular function, biological process, cellular component
- KEGG pathway mapping (metabolic pathways, signaling cascades)
- Pfam domain identification (conserved protein domains)
- InterPro family classification (protein families and domains)
- Cross-validation with phylogenetic analysis (function conservation)

Stage 6: Logic Tree Generation

- Construct hierarchical regulatory logic from TFBS arrangement
- Assign phase angles to regulatory inputs based on temporal order
- Verify phase closure requirement: $\sum \theta_i \equiv 0 \pmod{360}$
- Build Boolean logic functions from combinatorial TF binding
- Represent in WPE notation with field coupling operators

Stage 7: Orthogonal Closure Test

- Test all field pairs $\Phi_i \otimes \Phi_j$ for geometric stability
- Compute coupling strength: $|\Phi_i \otimes \Phi_j|$
- Verify no destructive interference (amplitude collapse)
- Ensure triad stability: three-way field interactions balanced
- Final validation of complete logical architecture

6.6.7 WPE Version 3 Dual-Strand Encoding

Biological logic encoded in complementary dual-strand notation:

Strand α (Alpha): Forward logical flow

$$\Xi\{\text{Logic}_i^+ = \text{Components} \supset [\text{Output}_n^+]\} \quad (76)$$

Operators: Ξ (integration kernel), \cdot (field container), \oplus (harmonic addition), \otimes (field coupling), \supset (implication), \int , \oint (domain integration)

Strand β (Beta): Complementary encoding

$$\triangleleft\{\text{Logic}_i^- \equiv \text{Components} \triangleright [\text{Output}_n^-]\}\trianglelefteq \quad (77)$$

Operators: $\triangleleft \cdot \trianglelefteq$ (complementary container), \equiv (equivalence), \circledast (node marker), \star (energy marker), \bowtie (coupling link)

Coherence Requirements:

1. Semantic equivalence: α and β describe same biological process
2. Structural complementarity: geometric duals (mirror symmetry)
3. Phase closure: $\sum \theta_\alpha + \sum \theta_\beta \equiv 0 \pmod{360}$

4. Energy conservation: $\sum \kappa_\alpha + \sum \kappa_\beta = 0$
5. Bidirectional translation: $\alpha \leftrightarrow \beta$ without information loss

Depth Keys: Spatial scale encoding through λ shells coupled with energy levels κ :

$$\lambda_1 : \text{Molecular} \quad \kappa \in [-6.5, -6.0] \quad (78)$$

$$\lambda_2 : \text{Cellular} \quad \kappa \in [-6.0, -5.5] \quad (79)$$

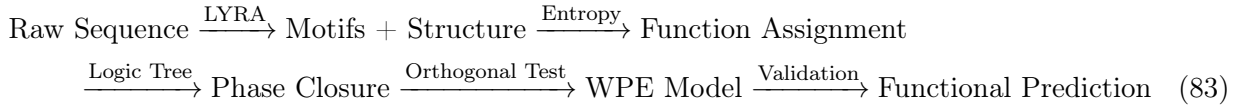
$$\lambda_3 : \text{Tissue} \quad \kappa \in [-5.5, -5.0] \quad (80)$$

$$\lambda_4 : \text{Organ} \quad \kappa \in [-5.0, -4.5] \quad (81)$$

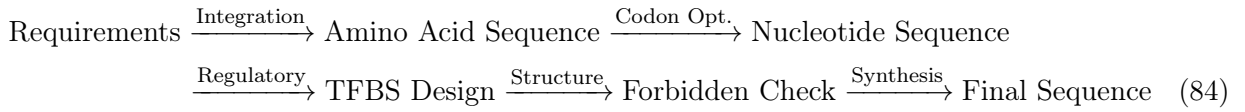
$$\lambda_5 : \text{Organismal} \quad \kappa \in [-4.5, -4.0] \quad (82)$$

6.6.8 Bidirectional DNA Flow

DNA → Function Pipeline:



Constraints → DNA Pipeline:



7 Layer 4: Robustness Mechanisms

7.1 Purpose and Scope

Layer 4 ($\kappa = -4.0$) encodes error detection, correction, redundancy, adaptation, and compensation mechanisms enabling biological systems to maintain function despite perturbations. Robustness is fundamental requirement—organisms face continuous environmental fluctuations, intrinsic stochasticity, replication errors, and aging damage. Without robustness mechanisms, biological systems would be fragile and short-lived.

7.2 Error Detection

DNA Mismatch Detection: DNA polymerase proofreading ($3' \rightarrow 5'$ exonuclease activity) detects incorrect base pairing. Error rate without proofreading: $\sim 10^{-5}$ per base. With proofreading: $\sim 10^{-7}$. Post-replication mismatch repair (MMR) further reduces to $\sim 10^{-10}$.

Damage Sensors: Specialized proteins detect DNA damage:

- UV-induced thymine dimers: detected by UV-DDB
- Oxidative damage (8-oxoguanine): detected by OGG1
- Double-strand breaks: detected by ATM, ATR kinases phosphorylating H2AX
- Replication stress: detected by checkpoint kinases (CHK1, CHK2)

Protein Misfolding Detection: Chaperone systems recognize exposed hydrophobic residues indicating misfolding. Heat shock proteins (HSP70, HSP90) bind unfolded proteins. GroEL/GroES (bacteria) encapsulates proteins for refolding attempts.

Metabolic Imbalance Sensors:

- AMP-activated protein kinase (AMPK): senses low ATP through AMP/ATP ratio
- mTOR: senses nutrient availability through amino acids
- HIF-1 α : senses hypoxia through oxygen-dependent degradation

Sensitivity Requirement: Detection systems must identify > 90% of errors to maintain low failure rate.

7.3 Error Correction

DNA Repair Pathways:

Base Excision Repair (BER): Repairs damaged bases.

1. Glycosylase removes damaged base (creating AP site)
2. AP endonuclease cleaves sugar-phosphate backbone
3. DNA polymerase fills gap
4. DNA ligase seals nick

Nucleotide Excision Repair (NER): Repairs bulky lesions (thymine dimers, chemical adducts).

1. Damage recognition (XPC-RAD23B complex)
2. Dual incision flanking lesion (~30 nucleotides)
3. Gap filling by DNA polymerase
4. Ligation

Mismatch Repair (MMR): Corrects replication errors.

1. Mismatch recognition (MutS homologs)
2. Strand discrimination via methylation or nick
3. Excision of error-containing strand
4. Resynthesis

Homologous Recombination (HR): Repairs double-strand breaks using sister chromatid template. High fidelity but requires homologous template (S/G2 phases).

Non-Homologous End Joining (NHEJ): Directly ligates broken ends. Fast but error-prone (small deletions/insertions). Primary pathway in G1.

Protein Quality Control:

Chaperone-Mediated Refolding: HSP70 binds hydrophobic regions of misfolded proteins, uses ATP hydrolysis for conformational changes promoting refolding. Multiple cycles attempted.

Proteasomal Degradation: Irreversibly misfolded proteins ubiquitinated and degraded by 26S proteasome. Prevents accumulation of toxic aggregates.

Autophagy: Damaged organelles (mitochondria, ER, peroxisomes) engulfed by autophagosomes and degraded in lysosomes. Maintains organelle quality control.

Apoptosis: Irreparable cellular damage triggers programmed cell death. Prevents propagation of mutations, especially in cancer prevention. Caspase cascade execution pathway.

Fidelity Requirement: Correction systems must achieve > 99.9% accuracy to maintain genome stability over organismal lifespan.

7.4 Redundancy

Gene Duplication: Paralogs provide functional backup. Whole-genome duplications in vertebrate evolution (2R hypothesis) created redundant gene pairs. Enables subfunctionalization (each paralog specializes) and neofunctionalization (one paralog gains new function).

Parallel Pathways: Multiple routes to critical products. Example: Glucose can be synthesized via gluconeogenesis from lactate, amino acids, or glycerol. ATP production via glycolysis (anaerobic) or oxidative phosphorylation (aerobic).

Organ Reserve: Most organs function at ~20-40% maximum capacity. Kidneys functional with single kidney. Liver regenerates from ~25% mass. Lung capacity far exceeds resting requirements. Reserve capacity enables survival despite partial damage.

Population Diversity: Genetic diversity within populations provides robustness against environmental change. No single pathogen or condition eliminates all individuals. Sexual reproduction maintains diversity through recombination.

Architectural Requirement: Critical functions require ≥ 2 independent pathways. Truly independent: not sharing rate-limiting steps or single points of failure.

7.5 Adaptation

Responses to persistent perturbations across timescales:

Allosteric Regulation (\sim milliseconds): Post-translational modification and conformational change. Phosphorylation activates/inhibits enzymes. Example: Phosphofructokinase inhibited by ATP (allosteric feedback).

Transcriptional Regulation (\sim minutes to hours): Gene expression changes. Heat shock increases HSP expression. Hypoxia induces HIF-1 α target genes (glycolytic enzymes, VEGF).

Phenotypic Plasticity (\sim days to weeks): Developmental responses to environment. Muscle hypertrophy from exercise. Altitude acclimatization (increased red blood cell production). Immune system adaptation to pathogens.

Evolution (\sim generations): Genetic change through selection. Antibiotic resistance in bacteria. Lactose tolerance in human populations with dairy farming history.

Each mechanism operates at characteristic timescale. Fast perturbations handled by allosteric regulation. Persistent changes require transcriptional or developmental adaptation. Multi-generational pressures drive evolution.

7.6 Compensation

Metabolic Compensation: Flux redistribution when pathways blocked. Warburg effect in cancer: glycolysis upregulation compensates for mitochondrial dysfunction. Amino acid catabolism increases during starvation.

Structural Compensation: Tissue remodeling. Cardiac hypertrophy compensates for increased workload. Bone density increases at stress points (Wolff's law). Collateral vessel formation after arterial blockage.

Functional Compensation: Altered activity levels. Remaining kidney hypertrophy after nephrectomy. Contralateral brain hemisphere assumes function after unilateral damage during development.

Behavioral Compensation: Modified actions. Favoring uninjured limb. Dietary changes in response to food aversion. Social support for impaired individuals.

8 Layer 5: Generative Engine

8.1 Purpose and Scope

Layer 5 ($\kappa = -4.5$, $\alpha = \phi \approx 1.618$) implements constraint integration and solution generation. This is the computational core performing optimization across all other layers. The golden ratio temporal scaling ($\alpha = \phi$) enables scale-free optimization without preferred timescale, allowing simultaneous integration of processes spanning femtoseconds to gigayears.

8.2 Constraint Integration

Collection: Gather all constraints from Layers 0–4:

$$C_{\text{substrate}} : \text{Bond energies, thermodynamics, geometry} \quad (85)$$

$$C_{\text{universal}} : \text{Allometry, homeostasis, hierarchy} \quad (86)$$

$$C_{\text{selection}} : \text{Evolution, self-organization, stochasticity} \quad (87)$$

$$C_{\text{information}} : \text{Sequences, regulation, DNA logic} \quad (88)$$

$$C_{\text{robustness}} : \text{Error detection/correction, redundancy} \quad (89)$$

Compatibility Checking: Verify no contradictions. Example contradictions:

- Reaction thermodynamically unfavorable ($\Delta G > 0$) without coupling mechanism
- Regulatory logic incomplete (missing required activator)
- Allometric scaling violated (heart rate incompatible with body mass)
- Phase closure failed ($\sum \theta \not\equiv 0 \pmod{360}$)

Priority Ordering: Weight constraints by $|\kappa|$ values:

$$w_i = e^{|\kappa_i|} \quad (90)$$

Substrate constraints ($\kappa = -7.0$) have weight $e^7 \approx 1100$. Selection constraints ($\kappa = -3.5$) have weight $e^{3.5} \approx 33$. Hard constraints enforced strictly; soft constraints act as preferences.

Solution Space Definition: Feasible region is intersection of all constraint sets:

$$\mathcal{F} = \bigcap_{i=1}^M F_i(\mathbf{x}) \quad (91)$$

where $\mathbf{x} \in \mathbb{R}^N$ represents system state (N variables, M constraints). Typically $M \gg N$ (overdetermined), yielding small feasible region or no exact solution.

8.3 Energy Minimization

Total energy functional:

$$E_{\text{total}}(\mathbf{x}) = \sum_i w_i E_i(\mathbf{x}) \quad (92)$$

Components:

$$E_{\text{thermo}} = \sum_{\text{reactions}} \Delta G_j \quad (93)$$

$$E_{\text{transport}} = \sum_{\text{gradients}} RT \ln(C_{\text{out}}/C_{\text{in}}) \quad (94)$$

$$E_{\text{synthesis}} = \sum_{\text{bonds}} \text{bond formation costs} \quad (95)$$

$$E_{\text{maintenance}} = \text{protein turnover} + \text{DNA repair} + \text{ion pumps} \quad (96)$$

Gradient Descent: Iteratively minimize energy:

$$\mathbf{x}_{t+1} = \mathbf{x}_t - \eta \nabla E(\mathbf{x}_t) \quad (97)$$

where η is learning rate. Ensures movement toward local minimum.

Simulated Annealing: Escape local minima through temperature schedule:

$$P(\text{accept worse solution}) = e^{-\Delta E/k_B T(t)} \quad (98)$$

Temperature $T(t)$ decreases over iterations: $T(t) = T_0 / \log(1 + t)$. Initially accepts uphill moves; gradually becomes deterministic gradient descent.

8.4 Information Maximization

Total information functional:

$$I_{\text{total}}(\mathbf{x}) = \sum_i w_i I_i(\mathbf{x}) \quad (99)$$

Subject to:

$$I_{\text{storage}} \leq H_{\text{Shannon}} \cdot N_{\text{symbols}} \quad (100)$$

$$I_{\text{transmission}} \leq B \log_2(1 + \text{SNR}) \quad (101)$$

$$I_{\text{computation}} \geq k_B T \ln 2 \text{ per bit (Landauer)} \quad (102)$$

Trade-Off with Energy: Information processing costs energy. High-fidelity transmission requires high SNR (costly). Dense information storage requires stable substrates (energetically expensive). Optimization balances these competing demands.

8.5 Iterative Refinement

```

1: Initialize candidate solution  $\mathbf{x}_0$ 
2: for iteration  $t = 1$  to  $T_{\max}$  do
3:   Apply all constraints:  $\mathbf{x}' = \text{Project}(\mathbf{x}_t, \{C_i\})$ 
4:   Evaluate fitness:  $F(\mathbf{x}') = -E(\mathbf{x}') + \lambda I(\mathbf{x}')$ 
5:   Compute gradient:  $\nabla F(\mathbf{x}')$ 
6:   Update:  $\mathbf{x}_{t+1} = \mathbf{x}' + \eta \nabla F + \text{Annealing noise}$ 
7:   Check convergence:  $|\mathbf{x}_{t+1} - \mathbf{x}_t| < \epsilon$ 
8:   if converged then
9:     return  $\mathbf{x}_{t+1}$ 
10:  end if
11: end for
12: return Best solution found

```

Convergence criteria: solution changes $< \epsilon$ over K consecutive iterations, all constraints satisfied within tolerance, energy/information objectives stable.

8.6 Multi-Scale Synthesis

Integration across spatial scales λ_1 (quantum) through λ_{10} (biosphere):

Consistency at Each Level: Solutions must satisfy constraints appropriate to each scale. Molecular level: bond geometries, reaction kinetics. Cellular level: metabolic fluxes, gene expression. Organismal level: allometric scaling, homeostasis.

Consistency Across Boundaries: Properties at scale n must emerge from scale $n - 1$. Cellular metabolism emerges from molecular enzyme kinetics. Organ function emerges from tissue organization. No "skipping levels"—all intermediate scales satisfied.

Upward Causation (Emergence): Lower-level interactions produce higher-level properties. Neuronal spiking \rightarrow network oscillations \rightarrow cognitive states. Protein interactions \rightarrow metabolic pathways \rightarrow cellular growth rate.

Downward Causation (Constraint): Higher-level states constrain lower-level dynamics. Blood pressure \rightarrow endothelial gene expression. Behavioral state \rightarrow neurotransmitter release patterns.

8.7 Temporal Integration

Fast Dynamics (10^{-3} to 10^0 s): Enzyme kinetics, ion channel gating, action potentials, muscle contraction. Steady-state assumption: fast processes equilibrate before slow processes change.

Intermediate Dynamics (10^3 to 10^6 s): Metabolic regulation, circadian rhythms, cell cycle, wound healing. Require explicit temporal integration, cannot assume steady-state.

Slow Dynamics (10^7 to 10^{10} s): Development, aging, seasonal cycles, population dynamics. Lower-frequency components in Fourier decomposition.

Evolutionary Dynamics (10^{10} to 10^{12} s): Selection, drift, speciation. Treated as boundary conditions for within-lifetime processes.

9 Layer 6: Layer Coupling

9.1 Purpose and Scope

Layer 6 ($\kappa = -4.0$) implements bidirectional coupling between all other layers, creating circular causation architecture. This transforms independent layer stack into self-consistent integrated system. Coupling ensures solutions simultaneously satisfy constraints from all layers—no layer can be optimized independently.

9.2 Coupling Architecture

Seven primary coupling relationships:

$$\mathcal{L}_0 \leftrightarrow \mathcal{L}_1 : \text{Substrate} \leftrightarrow \text{Universal} \quad (103)$$

$$\mathcal{L}_1 \leftrightarrow \mathcal{L}_2 : \text{Universal} \leftrightarrow \text{Selection} \quad (104)$$

$$\mathcal{L}_2 \leftrightarrow \mathcal{L}_3 : \text{Selection} \leftrightarrow \text{Information} \quad (105)$$

$$\mathcal{L}_3 \leftrightarrow \mathcal{L}_4 : \text{Information} \leftrightarrow \text{Robustness} \quad (106)$$

$$\mathcal{L}_4 \leftrightarrow \mathcal{L}_1 : \text{Robustness} \leftrightarrow \text{Universal} \quad (107)$$

$$\mathcal{L}_0 \leftrightarrow \mathcal{L}_5 : \text{Substrate} \leftrightarrow \text{Engine} \quad (108)$$

$$\mathcal{L}_5 \leftrightarrow \mathcal{L}_7 : \text{Engine} \leftrightarrow \text{Quantitative} \quad (109)$$

9.3 Bidirectional Coupling Explained

$\mathcal{L}_0 \mathcal{L}_1$: Substrate Universal

Forward: Chemistry determines which universal laws are implementable. Surface area-to-volume ratio (geometry, Layer 0) determines heat loss, constraining metabolic scaling (Layer 1).

Reverse: Universal laws select which chemical reactions occur in biological contexts. Not all thermodynamically favorable reactions occur—only those compatible with universal constraints (homeostasis, hierarchy, allometry).

$\mathcal{L}_1 \mathcal{L}_2$: Universal Selection

Forward: Universal laws constrain evolutionary trajectories. Allometric scaling limits viable body sizes. Hierarchical organization constrains developmental programs.

Reverse: Selection shapes which universal laws manifest. Different metabolic strategies (endothermy vs. ectothermy) produce different allometric exponents. Selection for robustness reinforces homeostatic mechanisms.

$\mathcal{L}_2 \mathcal{L}_3$: Selection Information

Forward: Selection acts on information structures. Beneficial mutations increase in frequency. Gene regulatory networks evolve under selection for robustness and evolvability.

Reverse: Information architecture constrains selection. Genetic architecture (linkage, pleiotropy, epistasis) determines accessible evolutionary paths. Developmental constraints limit phenotypic variation.

$\mathcal{L}_3 \mathcal{L}_4$: Information Robustness

Forward: Information content enables robustness. Redundant genes provide backup. Error-correcting codes in DNA repair. Regulatory networks buffer against noise.

Reverse: Robustness requirements shape information architecture. Need for error correction drives evolution of proofreading. Requirement for homeostasis shapes negative feedback loops in gene regulation.

$\mathcal{L}_4 \mathcal{L}_1$: Robustness Universal

Forward: Robustness mechanisms enable universal laws. DNA repair maintains genome stability required for universal constraints. Homeostatic mechanisms maintain conditions for allometric scaling.

Reverse: Universal laws define required robustness. Allometric scaling determines required error correction rates. Hierarchical organization requires buffering between levels.

This coupling creates stabilizing feedback: robustness enables universal laws, universal laws require robustness.

$\mathcal{L}_0 \mathcal{L}_5$: Substrate Engine

Forward: Chemistry provides primitives for engine. Molecular components, energy currencies (ATP), information carriers (DNA).

Reverse: Engine selects utilized chemistry. Not all possible molecules synthesized—only those satisfying integrated constraints.

$\mathcal{L}_5 \mathcal{L}_7$: Engine Quantitative

Forward: Engine invokes quantitative computations. Thermodynamic calculations, kinetic modeling, allometric predictions.

Reverse: Quantitative results constrain engine optimization. Numerical predictions must match experimental data within tolerances.

9.4 Over-Constrained Optimization

Circular coupling creates overdetermined system. With N free parameters and M constraints from all layers:

$$M = M_0 + M_1 + M_2 + M_3 + M_4 \gg N \quad (110)$$

Feasible region dramatically restricted:

$$\text{Volume}(\mathcal{F}) \ll \text{Volume}(\mathbb{R}^N) \quad (111)$$

Most random parameter combinations violate some constraint. Only carefully coordinated configurations satisfy all layers simultaneously. This explains why random mutations are typically deleterious—they violate multi-layer constraints.

9.5 Self-Consistency Requirements

Solutions must be self-consistent across all layers:

1. **Energetic consistency:** Energy budget from Layer 1 satisfied by metabolism from Layer 0
2. **Temporal consistency:** Timescale separation maintained across all processes
3. **Spatial consistency:** Hierarchical organization respected, no level-skipping
4. **Information consistency:** DNA sequence (Layer 3) encodes proteins satisfying substrate constraints (Layer 0)
5. **Regulatory consistency:** Gene networks (Layer 3) maintain homeostasis (Layer 1)
6. **Evolutionary consistency:** Current state (Layers 0–4) reachable from ancestral state via selection (Layer 2)
7. **Robustness consistency:** Error rates low enough (Layer 4) to maintain information fidelity (Layer 3)

Violation of any consistency condition indicates invalid solution.

10 Layer 7: Quantitative Computation

10.1 Purpose and Scope

Layer 7 ($\kappa = -5.5$) provides formulas, constants, molecular properties, and reaction parameters enabling quantitative predictions. This layer contains no constraints per se—rather, it implements computations required by other layers. Hard κ value reflects requirement that numerical predictions match experimental measurements.

10.2 Formula Library

Allometry:

$$\text{BMR} = 70 \cdot M^{0.75} \quad (\text{W}) \quad (112)$$

$$\text{HR} = 241 \cdot M^{-0.25} \quad (\text{beats/min}) \quad (113)$$

$$\text{LS} = 185.2 \cdot M^{0.24} \quad (\text{months}) \quad (114)$$

$$\text{SA} = k \cdot M^{2/3} \quad (115)$$

Thermodynamics:

$$\Delta G = \Delta H - T\Delta S \quad (116)$$

$$\Delta G = \Delta G^\circ + RT \ln Q \quad (117)$$

$$\Delta G^\circ = -RT \ln K_{\text{eq}} \quad (118)$$

$$k = A e^{-E_a/RT} \quad (119)$$

Kinetics:

$$v = \frac{V_{\max}[S]}{K_M + [S]} \quad (\text{Michaelis-Menten}) \quad (120)$$

$$v = \frac{V_{\max}[S]^n}{K_{0.5}^n + [S]^n} \quad (\text{Hill equation}) \quad (121)$$

$$v = \frac{V_{\max}[S]}{K_M(1 + [I]/K_i) + [S]} \quad (\text{competitive inhibition}) \quad (122)$$

Transport:

$$J = -D \frac{dC}{dx} \quad (\text{Fick's first law}) \quad (123)$$

$$D = \frac{k_B T}{6\pi\eta r} \quad (\text{Stokes-Einstein}) \quad (124)$$

$$r_{\text{parent}}^3 = \sum r_{\text{daughter}}^3 \quad (\text{Murray's law}) \quad (125)$$

$$\Delta P = \frac{8\eta LQ}{\pi r^4} \quad (\text{Poiseuille}) \quad (126)$$

Electrophysiology:

$$E = \frac{RT}{zF} \ln \frac{C_{\text{out}}}{C_{\text{in}}} \quad (\text{Nernst}) \quad (127)$$

$$V_m = \frac{RT}{F} \ln \frac{P_K[K^+]_{\text{out}} + P_{\text{Na}}[Na^+]_{\text{out}}}{P_K[K^+]_{\text{in}} + P_{\text{Na}}[Na^+]_{\text{in}}} \quad (\text{Goldman-Hodgkin-Katz}) \quad (128)$$

10.3 Constants Database

Table 4: Universal and Biological Constants

Constant	Symbol	Value
<i>Universal</i>		
Gas constant	R	8.314 J/(mol·K)
Boltzmann constant	k_B	1.381×10^{-23} J/K
Avogadro's number	N_A	6.022×10^{23} /mol
Planck constant	h	6.626×10^{-34} J·s
Faraday constant	F	96485 C/mol
Elementary charge	e	1.602×10^{-19} C
<i>Biological (Mammalian)</i>		
Body temperature	T	310 K (37°C)
Blood pH	–	7.4
ATP hydrolysis	ΔG_{ATP}	–30.5 kJ/mol (standard) –36.2 kJ/mol (cellular)

10.4 Molecular Database

Complete molecular properties for glycolysis reactants, products, cofactors. Example entries:

Glucose ($C_6H_{12}O_6$):

- Molecular weight: 180.16 g/mol
- $\Delta G_f^\circ = -917.2$ kJ/mol
- Typical cellular concentration: 5 mM (blood)

ATP:

- Molecular weight: 507.18 g/mol
- $\Delta G_{\text{hyd}} = -30.5$ kJ/mol (standard), –36.2 kJ/mol (cellular)

- Typical concentration: 5 mM

NAD^+/NADH :

- Standard reduction potential: $E^\circ = -0.32 \text{ V}$
- NAD^+/NADH ratio: ~ 700 (cytoplasm), ~ 8 (mitochondria)

10.5 Reaction Database

Complete glycolysis pathway (10 reactions) with parameters:

Reaction 1: Hexokinase

- Glucose + ATP \rightarrow G6P + ADP
- $\Delta G^\circ = -16.7 \text{ kJ/mol}$
- $\Delta G_{\text{cell}} = -33.5 \text{ kJ/mol}$
- $K_M(\text{Glc}) = 0.1 \text{ mM}$
- $k_{\text{cat}} = 300 \text{ s}^{-1}$
- Inhibition: G6P ($K_i = 0.1 \text{ mM}$)

Reaction 3: Phosphofructokinase (PFK)

- F6P + ATP \rightarrow F1,6BP + ADP
- $\Delta G_{\text{cell}} = -22.2 \text{ kJ/mol}$ (rate-limiting)
- Hill coefficient: $n = 2.0$ (cooperative)
- Inhibition: ATP ($K_i = 0.5 \text{ mM}$), citrate ($K_i = 2.5 \text{ mM}$)
- Activation: AMP ($K_a = 0.02 \text{ mM}$), F2,6BP ($K_a = 0.001 \text{ mM}$)
- Major control point

Reaction 10: Pyruvate Kinase

- PEP + ADP \rightarrow Pyruvate + ATP
- $\Delta G_{\text{cell}} = -16.7 \text{ kJ/mol}$
- Hill coefficient: $n = 1.8$

- Activation: F1,6BP (feedforward)
- Second commitment point

Net Glycolysis:

- Glucose + 2 NAD⁺ + 2 ADP + 2 P_i → 2 Pyruvate + 2 NADH + 2 ATP
- Net ATP yield: 2 per glucose
- Total $\Delta G \approx -85$ kJ/mol
- Efficiency: ~7.5% (61 kJ in ATP / 2840 kJ total combustion)

10.6 DNA Computation Procedures

Shannon Entropy:

$$H = - \sum_{x \in \{A,T,G,C\}} P(x) \log_2 P(x) \quad (129)$$

Recursive Collapse Depth: Iteratively compress sequence, count iterations to stabilization.

Fractal Harmonics: Autocorrelation at periods 3^n for $n = 1$ to 6.

Forbidden States: For k-mers: $F(k) = 1 - e^{-0.325k}$

Compression Ratio: Recursive WPE compression for sequences > 1000 bp, target $C_\infty \approx 5.88 : 1$.

Phase Closure: $\sum \theta \equiv 0 \pmod{360}$

Orthogonal Test: All pairs $\Phi_i \otimes \Phi_j$ tested for stability.

11 Validation Framework

11.1 Eight-Level Hierarchy

Validation proceeds hierarchically from substrate through quantitative accuracy. Solutions must pass all levels.

11.1.1 Level 1: Substrate Validation

Bond Energy Feasibility:

- All bonds within 10% of standard values

- C–C: 347 ± 35 kJ/mol
- C=O: 799 ± 80 kJ/mol
- Non-standard bonds require explicit verification

Molecular Geometry:

- Bond lengths within acceptable ranges ($\pm 10\%$)
- Bond angles correct for hybridization (± 15)
- Steric clashes: no atoms < 3 Å apart (excluding bonded)
- Ramachandran validation for proteins

Charge Balance:

- Total charge consistent with pH, ionization
- $|\sum q_i| < N/3$ (empirical heuristic)

Thermodynamic Feasibility:

- ΔG at physiological conditions (pH 7.0–7.4, 37°C, 150 mM ionic strength)
- Unfavorable reactions ($\Delta G > 0$) must be coupled or driven by gradients

Kinetic Accessibility:

- Rates achievable with enzyme concentrations < 1 mM
- $k_{\text{cat}}/K_M < 10^9 \text{ M}^{-1}\text{s}^{-1}$ (diffusion limit)

11.1.2 Level 2: Universal Constraints

Allometric Scaling:

- BMR within 20% of $70 \cdot M^{0.75}$
- HR within 20% of $241 \cdot M^{-0.25}$
- Surface area within 20% of $M^{2/3}$

Homeostasis Structure:

- Setpoint defined
- Sensor present and orthogonal (90° phase)
- Integrator opposes deviation (180° phase)
- Effector appropriate (270° phase)
- Negative feedback topology
- Stability: eigenvalues with negative real parts

Hierarchy:

- Proper scale ordering (no inversions)
- Adjacent-level coupling only
- No level-skipping in causal chains
- Emergence at appropriate levels

Temporal Separation:

- Factor ≥ 10 between adjacent timescales

Energy Budget:

- Total expenditure \leq available energy
- Efficiency $> 20\%$ (biological heuristic)

Information Bounds:

- Channel capacity within Shannon limit
- Bit operations respect Landauer limit

11.1.3 Level 3: Evolutionary Plausibility

Mutational Path:

- Accessible path from current state exists
- Fitness valleys $< 5\%$ of population can cross

Fitness Advantage:

- Selection coefficient s calculated
- Fixation probability $> 1\%$ for beneficial mutations

Phylogenetic Consistency:

- Compatible with evolutionary tree
- Robinson-Foulds distance $< 30\%$

11.1.4 Level 4: Information Encoding**Codon Usage:**

- CAI > 0.5
- Rare codons $< 10\%$
- Organism-appropriate preferences

Regulatory Network:

- All genes have promoters, terminators
- Logic tree present and coherent
- Noncoding scaffolds predicted

Phase Closure:

- $\sum \theta \equiv 0 \text{ mod } 360$
- All regulatory cycles close

Orthogonal Coupling:

- All field pairs $\Phi_i \otimes \Phi_j$ stable
- No destructive interference

Strand Coherence:

- Alpha and beta semantically equivalent
- Structural complementarity verified
- Bidirectional translation successful

11.1.5 Level 5: Robustness

Error Detection:

- Sensors present for mismatches, damage, misfolding, metabolic imbalance
- Sensitivity > 90%

Error Correction:

- DNA repair: BER, NER, MMR, HR, NHEJ pathways
- Protein quality control: chaperones, proteasome, autophagy
- Apoptosis for irreparable damage
- Fidelity > 99.9%

Redundancy:

- Critical functions have ≥ 2 independent pathways
- Pathways truly independent (no shared rate-limiting steps)

11.1.6 Level 6: Cross-Scale Consistency

Vertical Coupling:

- Upward causation (emergence) verified
- Downward causation (constraints) verified
- Timescale separation maintained

Horizontal Coupling:

- Spatial interactions appropriate
- Temporal synchronization where required

11.1.7 Level 7: Temporal Stability

Short-Term (10 seconds):

- No catastrophic failure
- No runaway dynamics
- Convergence to stable state

Medium-Term (developmental stages):

- All transitions successful
- Timeline appropriate for organism

Long-Term (evolutionary):

- Evolutionarily stable strategy
- Resistant to mutant invasion
- Population genetic stability

11.1.8 Level 8: Quantitative Accuracy

Thermodynamic:

- ΔG calculations within 10% of experimental
- Non-standard condition corrections applied

Kinetic:

- Rate constants within factor of 10 of measurements
- Enzyme parameters reasonable

DNA Information Metrics:

- Shannon entropy: 1.95–2.0 bits/symbol
- Compression ratio: 5.88 : 1 \pm 10% for sequences > 1000 bp

Forbidden State Compliance:

- $F(k)$ not exceeded
- Saturation levels appropriate

11.2 Validation Algorithm

```

1: function VALIDATECOMPLETE(solution)
2:   report  $\leftarrow \{\}$ 
3:   if NOT ValidateSubstrate(solution) then
4:     return (FAIL, report)
5:   end if
6:   if NOT ValidateUniversal(solution) then
7:     return (FAIL, report)
8:   end if
9:   if NOT ValidateEvolution(solution) then
10:    return (FAIL, report)
11:   end if
12:   if NOT ValidateInformation(solution) then
13:     return (FAIL, report)
14:   end if
15:   if NOT ValidateRobustness(solution) then
16:     return (FAIL, report)
17:   end if
18:   if NOT ValidateCoupling(solution) then
19:     return (FAIL, report)
20:   end if
21:   if NOT ValidateStability(solution) then
22:     return (FAIL, report)
23:   end if
24:   if NOT ValidateQuantitative(solution) then
25:     return (FAIL, report)
26:   end if
27:   return (PASS, report)
28: end function

```

Solutions must pass all eight levels sequentially. Early failure prevents wasted computation on invalid configurations.

12 Conclusion

The BioGenerative Cognition Crystal presents a constraint-based generative architecture for biological modeling fundamentally distinct from database-driven pattern matching or template-based systems. By encoding universal physical, chemical, biological, evolutionary, informational, and robustness constraints across seven hierarchical layers with bidirectional coupling, the framework generates complete biological solutions through simultaneous constraint satisfaction rather than

retrieval from pre-computed examples.

Version 2.0 integration of LYRA $^{\Theta\infty}$ DNA capabilities based on information physics enables bidirectional translation between nucleotide sequences and functional biological models through systematic seven-stage analysis and Wave Pattern Encoding notation. The framework treats DNA as symbolic substrate obeying information-theoretic principles (recursive collapse, fractal harmonics, forbidden states, compression limits) independent of biochemical interpretation, providing rigorous foundation for extracting biological logic from genomic sequences.

The circular causation architecture through bidirectional layer coupling creates over-constrained optimization requiring simultaneous satisfaction of constraints across all scales. This dramatically reduces solution space, explaining why biological systems occupy tiny fraction of theoretically possible configurations and why random mutations typically prove deleterious. Solutions must satisfy substrate physics (Layer 0), universal biological laws (Layer 1), evolutionary accessibility (Layer 2), information encoding including DNA (Layer 3), robustness requirements (Layer 4), through generative optimization (Layer 5), layer coupling (Layer 6), and quantitative accuracy (Layer 7).

The eight-level validation framework ensures solutions satisfy constraints from substrate chemistry through quantitative predictions, providing systematic quality control from first principles. This constraint-based generative paradigm represents potential shift in biological modeling from empirical description toward theoretical prediction, analogous to historical transitions in physics from geocentric to heliocentric models or from phlogiston to oxygen theory—not merely incremental improvement but fundamental reconceptualization of the explanatory framework.

References

- [1] Altschul, S.F., Gish, W., Miller, W., Myers, E.W., and Lipman, D.J. (1990). Basic local alignment search tool. *Journal of Molecular Biology*, 215(3):403–410.
- [2] Anderson, P.W. (1972). More is different. *Science*, 177(4047):393–396.
- [3] Atkins, P. and de Paula, J. (2010). *Atkins' Physical Chemistry*. Oxford University Press, 9th edition.
- [4] Banavar, J.R., Maritan, A., and Rinaldo, A. (1999). Size and form in efficient transportation networks. *Nature*, 399(6732):130–132.
- [5] Becskei, A. and Serrano, L. (2000). Engineering stability in gene networks by autoregulation. *Nature*, 405(6786):590–593.
- [6] Berman, H.M., Westbrook, J., Feng, Z., et al. (2000). The Protein Data Bank. *Nucleic Acids Research*, 28(1):235–242.
- [7] Billman, G.E. (2013). Homeostasis: The underappreciated and far too often ignored central organizing principle of physiology. *Frontiers in Physiology*, 4:200.

- [8] Bird, A. (2007). Perceptions of epigenetics. *Nature*, 447(7143):396–398.
- [9] Campbell, D.T. (1974). 'Downward causation' in hierarchically organised biological systems. In *Studies in the Philosophy of Biology*, pages 179–186. Springer.
- [10] Cannon, W.B. (1929). Organization for physiological homeostasis. *Physiological Reviews*, 9(3):399–431.
- [11] Crick, F.H. (1966). The genetic code—yesterday, today, and tomorrow. *Cold Spring Harbor Symposia on Quantitative Biology*, 31:3–9.
- [12] Darwin, C. (1859). *On the Origin of Species by Means of Natural Selection*. John Murray, London.
- [13] Davidson, E.H. (2006). *The Regulatory Genome: Gene Regulatory Networks in Development and Evolution*. Academic Press.
- [14] Dill, K.A. (1990). Dominant forces in protein folding. *Biochemistry*, 29(31):7133–7155.
- [15] Einstein, A. (1905). Über die von der molekularkinetischen Theorie der Wärme geforderte Bewegung von in ruhenden Flüssigkeiten suspendierten Teilchen. *Annalen der Physik*, 322(8):549–560.
- [16] Ferrell, Jr., J.E. (2002). Self-perpetuating states in signal transduction: positive feedback, double-negative feedback and bistability. *Current Opinion in Cell Biology*, 14(2):140–148.
- [17] Fick, A. (1855). Über diffusion. *Annalen der Physik*, 170(1):59–86.
- [18] Fisher, R.A. (1930). *The Genetical Theory of Natural Selection*. Clarendon Press, Oxford.
- [19] Frausto da Silva, J.J.R. and Williams, R.J.P. (1979). *The Biological Chemistry of the Elements: The Inorganic Chemistry of Life*. Oxford University Press.
- [20] Friedberg, E.C., Walker, G.C., Siede, W., Wood, R.D., Schultz, R.A., and Ellenberger, T. (2006). *DNA Repair and Mutagenesis*. ASM Press, 2nd edition.
- [21] Glickman, M.H. and Ciechanover, A. (2002). The ubiquitin-proteasome proteolytic pathway: destruction for the sake of construction. *Physiological Reviews*, 82(2):373–428.
- [22] Goldbeter, A. (2002). Computational approaches to cellular rhythms. *Nature*, 420(6912):238–245.
- [23] Goldman, D.E. (1943). Potential, impedance, and rectification in membranes. *Journal of General Physiology*, 27(1):37–60.
- [24] Gurdon, J.B. and Bourillot, P.Y. (1999). Morphogen gradient interpretation. *Nature*, 413(6858):797–803.

- [25] Haldane, J.B.S. (1927). A mathematical theory of natural and artificial selection, part V: selection and mutation. *Mathematical Proceedings of the Cambridge Philosophical Society*, 23(7):838–844.
- [26] Hartl, F.U., Bracher, A., and Hayer-Hartl, M. (2011). Molecular chaperones in protein folding and proteostasis. *Nature*, 475(7356):324–332.
- [27] Hill, A.V. (1910). The possible effects of the aggregation of the molecules of haemoglobin on its dissociation curves. *The Journal of Physiology*, 40(Suppl):iv–vii.
- [28] Iyer, R.R., Pluciennik, A., Burdett, V., and Modrich, P.L. (2006). DNA mismatch repair: functions and mechanisms. *Chemical Reviews*, 106(2):302–323.
- [29] Jones, D.T., Taylor, W.R., and Thornton, J.M. (1992). A new approach to protein fold recognition. *Nature*, 358(6381):86–89.
- [30] Jumper, J., Evans, R., Pritzel, A., et al. (2021). Highly accurate protein structure prediction with AlphaFold. *Nature*, 596(7873):583–589.
- [31] Kanehisa, M. and Goto, S. (2000). KEGG: Kyoto Encyclopedia of Genes and Genomes. *Nucleic Acids Research*, 28(1):27–30.
- [32] Kimura, M. (1968). Evolutionary rate at the molecular level. *Nature*, 217(5129):624–626.
- [33] Kirkpatrick, S., Gelatt, C.D., and Vecchi, M.P. (1983). Optimization by simulated annealing. *Science*, 220(4598):671–680.
- [34] Kitano, H. (2002). Systems biology: a brief overview. *Science*, 295(5560):1662–1664.
- [35] Kleiber, M. (1947). Body size and metabolic rate. *Physiological Reviews*, 27(4):511–541.
- [36] Kouzarides, T. (2007). Chromatin modifications and their function. *Cell*, 128(4):693–705.
- [37] Kunkel, T.A. and Bebenek, K. (2000). DNA replication fidelity. *Annual Review of Biochemistry*, 69:497–529.
- [38] Landauer, R. (1961). Irreversibility and heat generation in the computing process. *IBM Journal of Research and Development*, 5(3):183–191.
- [39] Lide, D.R. (2004). *CRC Handbook of Chemistry and Physics*. CRC Press, 85th edition.
- [40] Lynch, M. (2010). Evolution of the mutation rate. *Trends in Genetics*, 26(8):345–352.
- [41] McNab, B.K. (2002). *The Physiological Ecology of Vertebrates: A View from Energetics*. Cornell University Press.
- [42] Meinhardt, H. (1982). *Models of Biological Pattern Formation*. Academic Press, London.
- [43] Michaelis, L. and Menten, M.L. (1913). Die kinetik der invertinwirkung. *Biochemische Zeitschrift*, 49:333–369.

- [44] Mizushima, N., Levine, B., Cuervo, A.M., and Klionsky, D.J. (2008). Autophagy fights disease through cellular self-digestion. *Nature*, 451(7182):1069–1075.
- [45] Monod, J., Wyman, J., and Changeux, J.P. (1965). On the nature of allosteric transitions: a plausible model. *Journal of Molecular Biology*, 12(1):88–118.
- [46] Murray, C.D. (1926). The physiological principle of minimum work: I. The vascular system and the cost of blood volume. *Proceedings of the National Academy of Sciences*, 12(3):207–214.
- [47] Nelson, D.L. and Cox, M.M. (2008). *Lehninger Principles of Biochemistry*. W.H. Freeman, 5th edition.
- [48] Nernst, W. (1888). Zur kinetik der in lösung befindlichen körper. *Zeitschrift für Physikalische Chemie*, 2:613–637.
- [49] Nicolis, G. and Prigogine, I. (1977). *Self-Organization in Nonequilibrium Systems*. Wiley, New York.
- [50] Noble, D. (2006). *The Music of Life: Biology Beyond the Genome*. Oxford University Press.
- [51] Noble, D. (2012). A theory of biological relativity: no privileged level of causation. *Interface Focus*, 2(1):55–64.
- [52] Novikoff, A.B. (1945). The concept of integrative levels and biology. *Science*, 101(2618):209–215.
- [53] Ohno, S. (1970). *Evolution by Gene Duplication*. Springer-Verlag, Berlin.
- [54] Orth, J.D., Thiele, I., and Palsson, B.Ø. (2010). What is flux balance analysis? *Nature Biotechnology*, 28(3):245–248.
- [55] Pauling, L. (1931). The nature of the chemical bond. Application of results obtained from the quantum mechanics and from a theory of paramagnetic susceptibility to the structure of molecules. *Journal of the American Chemical Society*, 53(4):1367–1400.
- [56] Peng, C.K., Buldyrev, S.V., Goldberger, A.L., et al. (1992). Long-range correlations in nucleotide sequences. *Nature*, 356(6365):168–170.
- [57] Ptashne, M. and Gann, A. (2004). *Genes and Signals*. Cold Spring Harbor Laboratory Press.
- [58] Schirmer, T. and Evans, P.R. (1990). Structural basis of the allosteric behaviour of phosphofructokinase. *Nature*, 343(6254):140–145.
- [59] Schmitt, A.O. and Herzl, H. (1997). Estimating the entropy of DNA sequences. *Journal of Theoretical Biology*, 188(3):369–377.
- [60] Shannon, C.E. (1948). A mathematical theory of communication. *Bell System Technical Journal*, 27(3):379–423.

- [61] Simon, H.A. (1962). The architecture of complexity. *Proceedings of the American Philosophical Society*, 106(6):467–482.
- [62] Sinden, R.R. (1994). *DNA Structure and Function*. Academic Press, San Diego.
- [63] Stelling, J., Sauer, U., Szallasi, Z., Doyle III, F.J., and Doyle, J. (2004). Robustness of cellular functions. *Cell*, 118(6):675–685.
- [64] Strahl, B.D. and Allis, C.D. (2000). The language of covalent histone modifications. *Nature*, 403(6765):41–45.
- [65] Taylor, J.S. and Raes, J. (2004). Duplication and divergence: the evolution of new genes and old ideas. *Annual Review of Genetics*, 38:615–643.
- [66] Teusink, B., Passarge, J., Reijenga, C.A., et al. (2000). Can yeast glycolysis be understood in terms of in vitro kinetics of the constituent enzymes? Testing biochemistry. *European Journal of Biochemistry*, 267(17):5313–5329.
- [67] Turing, A.M. (1952). The chemical basis of morphogenesis. *Philosophical Transactions of the Royal Society of London B*, 237(641):37–72.
- [68] Tyson, J.J., Chen, K.C., and Novak, B. (2003). Sniffers, buzzers, toggles and blinkers: dynamics of regulatory and signaling pathways in the cell. *Current Opinion in Cell Biology*, 15(2):221–231.
- [69] Venter, J.C., Adams, M.D., Myers, E.W., et al. (2001). The sequence of the human genome. *Science*, 291(5507):1304–1351.
- [70] Voss, R.F. (1992). Evolution of long-range fractal correlations and 1/f noise in DNA base sequences. *Physical Review Letters*, 68(25):3805–3808.
- [71] West, G.B., Brown, J.H., and Enquist, B.J. (1997). A general model for the origin of allometric scaling laws in biology. *Science*, 276(5309):122–126.
- [72] West-Eberhard, M.J. (2003). *Developmental Plasticity and Evolution*. Oxford University Press.
- [73] Wolpert, L. (1969). Positional information and the spatial pattern of cellular differentiation. *Journal of Theoretical Biology*, 25(1):1–47.
- [74] Wright, S. (1931). Evolution in Mendelian populations. *Genetics*, 16(2):97–159.
- [75] Yuh, C.H., Bolouri, H., and Davidson, E.H. (1998). Genomic cis-regulatory logic: experimental and computational analysis of a sea urchin gene. *Science*, 279(5358):1896–1902.